External Magnetic Fields Effect on Harmonics Measurements with Rogowski coils

Alessandro Mingotti, Federica Costa, Lorenzo Peretto and Roberto Tinarelli
Department of Electric, Electronic and Information Engineering
University of Bologna
Bologna, Italy
alessandro.mingotti2, federica.costa13, lorenzo.peretto, roberto.tinarelli3@unibo.it

***Abstract*—The power quality (PQ) problem is spreading among the distribution network (DN) since intelligent electronic devices (IED) are being installed. Their presence is crucial because they introduce several benefits for the network observability and management. However, the consequent power quality degradation has to be seriously tackled. To this purpose, measurement instruments should be capable of measuring the electrical quantities even in presence of distortion. Furthermore, the new added distortion has to be summed to the typical influence factors affecting the measurement instruments (like temperature, electromagnetic fields, humidity, etc.). Therefore, this paper presents a study on a specific low-power current transformer (LPCT), the Rogowski coil. In detail, the influence of external magnetic fields, on the Rogowski accuracy performance, is evaluated when the device is measuring distorted signals (with an increasing level of distortion). The aim is to study the combined effect of the magnetic fields and of the distorted currents on the measurement performance of a Rogowski coil. Therefore, an ad-hoc measurement setup and tests are developed in this work to assess 3 off-the-shelf Rogowski coils. From the results it can be concluded that the presence of external magnetic fields does not influence the harmonics evaluation, but it does influence the evaluation of the 50 Hz component.**

Keywords*—Low power instrument transformer, Rogowski coil, LPCT, distorted signals, power quality, external magnetic fields, influence quantity.

I. Introduction

The spread of Intelligent Electronic Devices (IEDs) is increasing every day. This results into two main consequences: (i) the increased complexity of the network and of its equipment; (ii) the effect on the power quality level due to the IED presence. The former consequence is mainly solved by System Operators (SOs) who have to manage and control the network. However, their work is typically facilitated by control algorithms and new techniques developed by researchers [1-3].

The SO aim is to maintain the voltage quality within the limits defined in the IEC 50160 [4]. Therefore, the second consequence becomes highly important and has to be properly addressed. To this purpose, the new generation of Low-Power Instrument Transformers (LPITs) [5], which is replacing the legacy inductive one, has the characteristic for facing the power quality problems. In fact, they typically feature reduced dimensions, wider bandwidth, higher immunity to external influence quantities, compared to the inductive instrument transformers (ITs).

Therefore, this paper studies a particular kind of LPIT, the Rogowski coil. Its high rate of adoption in the distribution network (DN) is clearly justified by its flexibility, ease of installation, wide bandwidth, etc.

Aim of this work is to assess the Rogowski performance, in presence of external magnetic fields, when it is measuring distorted currents. Of course, both influence quantities and distorted currents are topics well stressed in literature as far as the Rogowski is involved. In particular, [6-8] treat the harmonic analysis and measurement issues related to Rogowski coils, suggesting countermeasures. In [9-12], instead, the effect of influence quantities like temperature, geometry, magnetic fields, etc., is studied.

The added value of this work is to assess the change in the Rogowski accuracy performance when the external magnetic field is affecting a Rogowski coil measuring a distorted current.

What follows is structured as: Section II briefly describes the working principle of a Rogowski coil. The measurement setup and the experimental tests developed within this work are presented in Section III and IV, respectively. Finally, Section V and VI provides the results and the conclusion of the work, respectively.

II. Theoretical Framework

A. Rogowski coils operating principle

Rogowski coils are low-power current transformers (LPCTs) which are based on the same working principle as conventional iron-core current transformers (CTs).

What makes a difference between these two is that Rogowski coils are wound over a non-magnetic core, typically an air-core. Its peculiarity is that such core cannot saturate, resulting in a linear behavior devoid of saturation issues.

Rogowski coils are placed around a conductor in which the unknown current (i) has to be measured.

The schematic of an LPCT is depicted in Fig. 1. In it, the cross-section S and the radius R of the device can be distinguished.

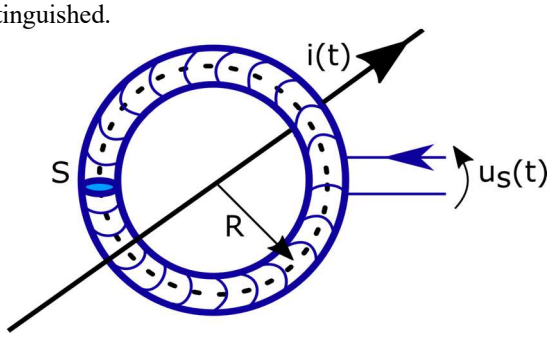

Fig. 1. Rogowski coil structure.

The output voltage u_s is proportional to the rate of change of the measured current i:

The 19NRM05 project has received funding from the EMPIR programme co-financed by the Participating States and from the European Union's Horizon 2020 research and innovation programme".

$$u_s(t) = -M\frac{di(t)}{dt}, \quad (1)$$

where M is the mutual inductance between the considered conductors.

As clearly indicated in (1), the phase angle between the Rogowski coil primary current and the secondary voltage is ideally $\pi/2$. Nevertheless, this value differs from the ideal one by an angle φ introduced by the coil parasitic parameters.

As the objective of this work involves the study of the performances of Rogowski coils under the influence of external magnetic fields, it is worth marking some further remarks about the structure of the considered LPCTs.

In fact, owing to the weak coupling between primary and secondary windings, Rogowski coils are designed in such a way that the undesirable influence of external conductors is minimized. For this reason, two wire loops are typically connected in electrically opposite directions which helps in cancelling the electromagnetic fields coming from the outside of the coil loop.

External magnetic fields as an influence quantity have already been considered in the relevant Standards, where a specific test has been designated to verify the influence of other phases on the accuracy of LPCTs [13].

The difference of both ratio and phase errors between measurements at the rated conditions and in presence of external fields shall be within 1/3 of the error limits of the relevant accuracy class [13].

In the next section, the measurement setup adopted for performing tests is described.

III. Measurement Setup

Fig. 2 shows the developed measurement setup. Its components are:

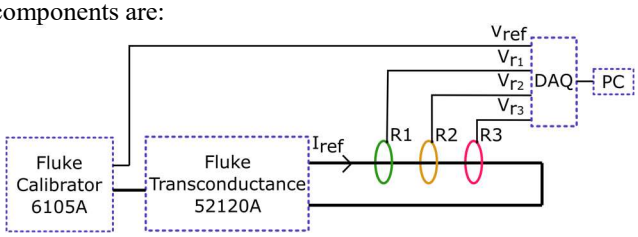

Fig. 2. Measurement Setup.

- Calibrator. Fluke 6105A controlling the transconductance Fluke 52120A is used to produce a reference primary current (I_{ref}), either sinusoidal or distorted. The calibrator accuracy characteristics are listed in Table I. The values in the table refers to the performance of the transconductance when controlled with the calibrator.

TABLE I. Calibrator Performance Specifications

Frequency	Current Accuracy		
	% of output	*% of range*	*Phase Angle*
DC	0.012	0.008	-
10 Hz to 69 Hz	0.009	0.002	0.005 °
69 Hz to 180 Hz			0.009 °
180 Hz to 450 Hz			0.020 °
450 Hz to 850 Hz			0.035 °
850 Hz to 3 kHz	0.040	0.004	0.250 °
3 kHz to 6 kHz			0.500 °

- Data AcQuisition board (DAQ). NI 9238 DAQ board is used to acquire the voltage measures. They are the reference voltage provided by the calibrator (V_{ref}), used as phase reference, and the three output voltages measured by the Rogowski coils (V_{r1}, V_{r2}, V_{r3}). The DAQ features a 24-bit analog-to-digital converter, an operating voltage range of ± 500 mV, simultaneous sampling at a maximum of 50 (kS/s)/ch, and an input impedance >1 GΩ (not specified if holds for a specific frequency).
- Rogowski coils. Three off-the-shelf Rogowski coils (R1, R2, R3) from different manufacturers, represented with different colors in Fig. 2, are used to perform tests. Their characteristics are presented in Table II. The voltage output in the table typically refers to the 50-60 Hz usage. However, in the Rogowski data sheets such information was not clearly indicated.

TABLE II. Rogowski Coils Rated Data

Info	Rogowski Coil		
	R1	*R2*	*R3*
Voltage output [mV/kA]	100	100	100
Frequency range [Hz]	20-5k	1 – 50k	50 – 60
Accuracy [%]	± 1	± 0.5	± 1
Linearity [%]	± 0.2	± 0.2	± 0.2
Position sensibility [%]	± 2 max	< 0.5 center < 1 sides	± 3 sides
External field [%]	± 0.5 max	Not given	± 2
Temperature range [°C]	-20 to +70	-40 to +80	-20 to +80

IV. Experimental Tests

In this Section, the experimental tests performed on the measurement setup illustrated in Fig. 2 and detailed in Section III are presented. This Section intends to present the measurement conditions and the evaluated parameters obtained from the preliminary assessments.

A. Testing conditions and configurations

According to the setup shown in Fig. 2, the combination of Fluke Calibrator and Transconductance is used to generate a reference current (I_{ref}) which is set equal to 100 A for all tests.

The three commercial Rogowski coils (R1, R2, R3) are wrapped around the conductor in which I_{ref} is flowing. Their output voltages, V_{r1}, V_{r2}, V_{r3}, are acquired using the NI 9238 DAQ board.

It is also worth noting that a reference voltage (V_{ref}) generated in the calibrator and equal to 500 mV is also acquired on one of the 4 channels of the DAQ. This signal aims at providing the phase reference needed to assess the phases of the Rogowski coils under test.

All the acquired signals are post-process in a PC using LabVIEW and MATLAB environments. A Fourier analysis is performed over 10000 Samples acquired at a sampling rate of 50000 (Samples/s)/ch, corresponding to an observation window of 200 ms. For each test 100 measurements are performed.

The tests described in Sections IV-B and -C are performed for all three Rogowski coils loaded with their rated burden (2 MΩ, see [5]). Furthermore, two positioning configurations are implemented. The first testing condition consists in placing the primary conductor perfectly centered with respect to the Rogowski coils' symmetry axes. This configuration, from here on after, is referred to as T1, for the sake of brevity. Results obtained from T1 configuration will be considered as a reference for the other configuration.

The second testing arrangement, instead, intends to study the effects of external magnetic fields due to proximity effects on the sensors when an external conductor is adjacent to it. The current value in the external conductor is the same as that in the main conductor. It is worth underlying that, even in this second configuration, the conductor is still centered with respect to the sensors' axes. This configuration, from here on after, is referred to as T2.

The two different configurations, resulting into two variations of the measurement setup, are illustrated respectively in Fig. 3 (a, b). For both figures, the Rogowski coil is represented in green, the solid black line represents the primary conductor in which a current I_{ref} is flowing, and the two dotted red lines represent the symmetry axes of the sensor.

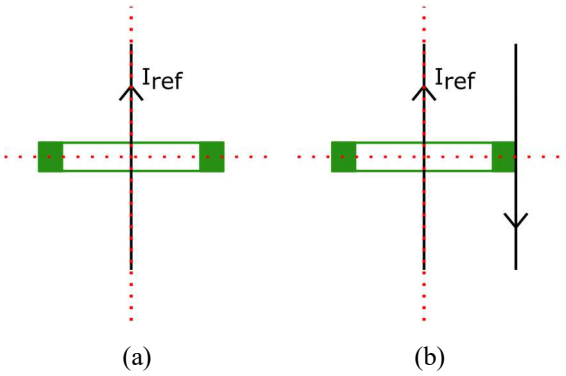

Fig. 3. Rogowski coil tests: (a) centered position (T1) and (b) effect of adjacent magnetic fields (T2).

In what follows the characteristics of the current injected through the primary conductor are detailed and distinguished between sinusoidal (Section B) and distorted signals (Section C).

B. Sinusoidal Tests

In these tests a pure sinusoidal current of 100 A RMS at 50 Hz (I_{ref}) is applied. The specifications illustrated in Section IV A hold for these tests. To evaluate the performances of the three sensors, the following errors are used:

a) Ratio error ε: it is calculated according to [5] as:

$$\varepsilon\,(\%) = \frac{K_r U_s - I_p}{I_P} \times 100, \qquad (2)$$

where K_r is the rated transformation ratio, I_p is the RMS value of the primary current and U_s is the RMS value of the secondary voltage (both extracted as the 50 Hz component of the signal).

This error is computed for all 3 Rogowski coils and for both configurations T1 and T2 to evaluate the difference in the two cases.

b) Phase error φ_e: in order to compute this error the reference voltage (V_{ref}) described in the previous Section III is used as a phase reference. This signal is used to compute the phase displacement introduced by the sensors which is theoretically equal to $\pi/2$, as shown in (1).

The phase error φ_e is computed according to [5] as:

$$\varphi_e = \varphi_s - \varphi_p, \qquad (3)$$

where φ_s is the secondary phase and φ_p is the primary one. Analogously to ε, φ_e is calculated for both T1 and T2 configurations.

C. Harmonic Tests

For these set of tests, using configurations T1 and T2, a rated current of 100 A RMS is injected via the calibrator and the transconductance. Superimposed to the 50 Hz component there are several combinations of harmonics (according to [14]).

Four different tests, referred to as A to D, are performed with an increasing harmonic content as specified in Table III. In particular, from left to right, there is: the name of the test, the order h of the considered harmonic, the percentage of the amplitude of the h-th harmonic with respect to the 50 Hz component ($h_{\%}$), the corresponding amplitude of the harmonic (I_h), the reference THD set by the calibrator (THD_{cal}) and regarded as a reference, and the actual RMS of the reference current I_{ref}, provided by the calibrator when setting 100 A.

TABLE III. LIST OF TESTS PERFORMED WITH HARMONICS

Test Name	h [/]	$h_{\%}$ [%]	I_h [A]	THD_{cal} [%]	I_{ref} [A]
A	3	4	4	4.8	99.8864
	11	2	2		
	17	1.5	1.5		
	23	0.6	0.6		
	35	0.3	0.3		
B	3	4	4	6.8	99.7727
	5	4	4		
	11	2	2		
	13	2	2		
	17	1.5	1.5		
	19	1.5	1.5		
	23	0.6	0.6		
	25	0.6	0.6		
	35	0.3	0.3		
	37	0.3	0.3		
C	3	4	4	8.3	99.6589
	5	4	4		
	7	4	4		
	11	2	2		
	13	2	2		
	15	2	2		
	17	1.5	1.5		
	19	1.5	1.5		
	21	1.5	1.5		
	23	0.6	0.6		
	25	0.6	0.6		
	27	0.6	0.6		
	35	0.3	0.3		
	37	0.3	0.3		
	39	0.3	0.3		
D	3	4	4	9.2	99.5764
	5	4	4		
	7	4	4		
	9	4	4		
	11	2	2		
	13	2	2		

	15	2	2		
	17	1.5	1.5		
	19	1.5	1.5		
	21	1.5	1.5		
	23	0.6	0.6		
	25	0.6	0.6		
	27	0.6	0.6		
	29	0.6	0.6		
	35	0.3	0.3		
	37	0.3	0.3		
	39	0.3	0.3		
	41	0.3	0.3		

These tests aim at assessing the performances of the Rogowski coils when it is simultaneously affected by a distorted current and by external magnetic fields. The attained results are used to calculate the following parameters:

a) Harmonic currents in [A]: performing the Fourier analysis on the output signal, the measured harmonic currents are evaluated and compared with respect to their reference values (I_h) set in the calibrator to assess the distortion introduced by the sensors.

b) THD: the harmonic content is used to compute the THD as:

$$THD = \frac{\sqrt{\sum_{h=2}^{N} {I_{h,RMS}}^2}}{I_{1,RMS}} \times 100, \qquad (4)$$

which is then compared to its reference value measured by the calibrator (THD_{cal}). In (4), $I_{1,RMS}$ is the 50 Hz component of the current I_{ref}, $I_{h,RMS}$ is the h-harmonic current, and N is the number of harmonic components.

c) Ratio error ε : the ratio error is computed according to Eq. (2).

d) Phase error φ_e: the phase error is computed according to Eq. (3).

All these parameters are computed for both T1 and T2 configurations and presented in the next section. Note, ratio and phase error have been calculated, even in distorted conditions, only for the 50 Hz component.

V. Test Results

In this Section the most significant results obtained from the tests illustrated in the previous Section IV are presented in the same order as they were introduced.

Fig. 4 presents the results obtained from Test D. This test, according to Table III, comprises the highest number of harmonics.

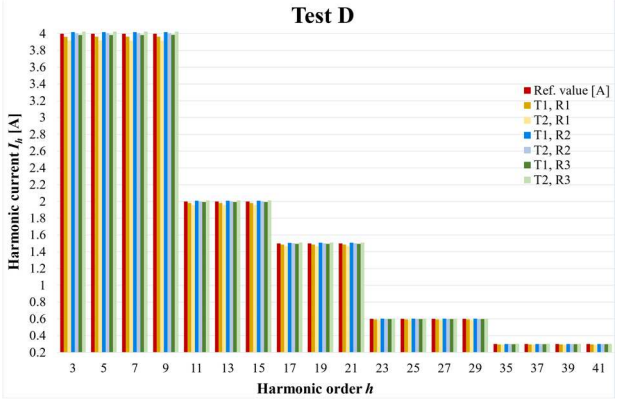

Fig. 4. Measured harmonic currents I_h in [A] as a function of the harmonic order h for the three Rogowski coils (R1, R2, R3) in configurations T1 and T2.

The figure presents the measured harmonic currents I_h in [A] as a function of the harmonic order h. The data represented with red color refer to the harmonic current set in the calibrator (see Table III) and have to be regarded as a reference.

In the same figure, darker colors represent tests performed in configuration T1. Respectively dark yellow, blue and green illustrate the results of Rogowski coils R1, R2 and R3. Following the same rationale, lighter colors present the results of Rogowski coils R1, R2 and R3 (yellow, blue and green, respectively) in configuration T2.

As depicted in Fig. 4, it is evident that the measured harmonic currents I_h by the three Rogowski coils under test are not strongly affected neither by the sensors themselves nor by the presence of external magnetic fields. Indeed, comparable results are obtained for all sensors and in both T1 and T2 configurations. A worsening in the estimation of harmonic content is present for low-order harmonics up to the 9th. Results for the harmonic configurations A to C are not presented, for the sake of brevity, because fully aligned with what above described.

The second parameter which has been evaluated is the THD. Fig. 5 shows the THD obtained applying Eq. (4) using the current components extracted with the FFT.

The graph presents the results obtained in all tests, namely A, B, C and D, for the three Rogowski coils and in both configurations T1 and T2.

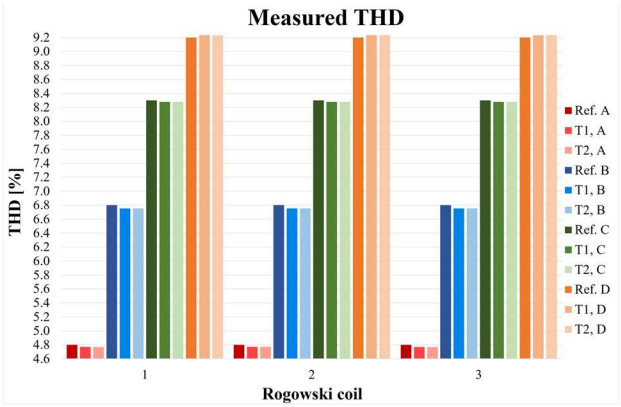

Fig. 5. Measured THD for the three Rogowski coils (1, 2, 3) in Tests A to D and in configurations T1 and T2.

Red, blue, green and yellow color bars respectively refer to Test A, B, C and D whose reference THD value is presented in Fig. 5 with the darkest shade, and it corresponds to the value shown in Table III, Section IV (THD_{cal}).

In Fig. 5, the two lighter colors, presented in all four test cases, respectively refer to the THD obtained using configurations T1 and T2.

The results shown in the graph of Fig. 5 confirm what has been previously observed in Fig. 4, meaning that the estimation of harmonic current components is not strongly affected by the intensity of the harmonic content (Tests A to D do not play any major role in this evaluation) nor by the presence of an external magnetic field affecting the primary conductor. Therefore, considering the negligible variation of the measured parameters, no zoomed pictures of the results has been reported for the sake of brevity.

Fig. 6 shows the measured ratio errors ε computed according to Eq. (2).

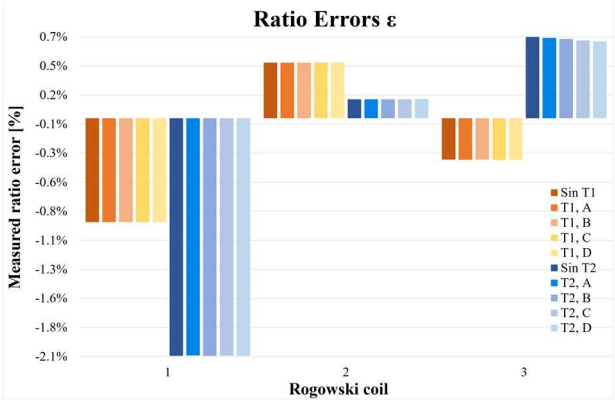

Fig. 6. Ratio error results for the three Rogowski coils (1, 2, 3) in sinusoidal and distorted conditions (Tests A to D) and in configurations T1 and T2.

The results shown in Fig. 6 depict both the ratio errors measured in pure sinusoidal conditions (darkest color) and the ones obtained in presence of high harmonic content (lighter colors), namely in Tests A to D, for all three Rogowski coils. The orange shades present the outcomes obtained from configuration T1, whereas the blue ones the results from configuration T2.

No reference color bar has been shown as, clearly, an ideal Rogowski coil should have an ε approaching zero.

The graph illustrated in Fig. 6 provides some interesting results regarding the behavior of the three devices under test in presence of external magnetic fields.

Precisely, it could be noticed that the presence of an external field in the nearby of the primary conductor not always implies a worsening in the performance of the sensor. Indeed, R2 ε reduces more than 50 % in configuration T2 with respect to its reference case T1 (note that all ε values presented refer to the 50 Hz component).

On the other hand, R1 results show that T2 configuration played a major role in the deterioration of the performances, as the ε has more than doubled with respect to T1.

Finally, R3 presents another different behavior compared to the other two devices under test. In this case, not only did the ε worse its performance in T2, but it also changed sign.

A final remark concerns the harmonic content present in the four tests A to D which have been carried out. It is worth noting that the number of harmonics does not strongly influence the ε for all three Rogowski coils R1, R2 and R3. Indeed, what has been measured for the pure sinusoidal case is comparable with all four harmonic tests.

Lastly, Fig. 7 shows φ_e in [rad] obtained applying both a pure sinusoidal waveform and in the four distorted Tests A to D.

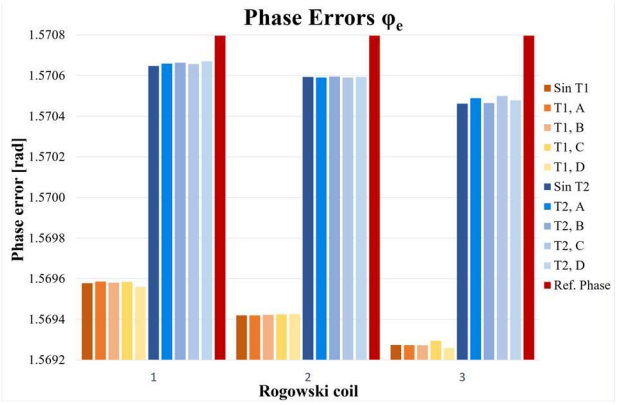

Fig. 7. Phase error results for the three Rogowski coils (1, 2, 3) in sinusoidal and distorted conditions (Tests A to D) and in configurations T1 and T2.

The color code used in Fig. 6 is replicated in Fig. 7 as well, for the sake of clarity. In addition, in Fig. 7 a red-colored indicator has been added to represent the ideal $\pi/2$ phase displacement introduced by the coil.

Some of the considerations previously done for Fig. 6 hold true also in this case, namely the configuration T2 tends to strongly affect φ_e with respect to T1 case.

Lastly, φ_e does not significantly vary depending on the intensity of the harmonic content, albeit higher fluctuations are visible in case of R3.

Having analyzed all the achieved results, it can be concluded that the amount of the harmonic content does not significantly impact the evaluation of harmonic currents, the THD, ε, and φ_e. However, it has been highlighted that on the one hand the harmonic evaluation is not affected by the presence of magnetic fields. On the contrary, the evaluation of the 50 Hz components is strongly affected by it, leading to a worsening of the Rogowski performances.

VI. Conclusions

This work presents a study involving the evaluation of the harmonic content by Rogowski coils both in rated conditions and in presence of external magnetic fields.

The latter type of tests is taken into account as the Standards do not provide specific information concerning the evaluation of the harmonic content in presence of nearby magnetic fields.

The results have shown that the intensity of harmonic content does not play any major role in the estimation of ratio and phase errors, instead the presence of magnetic fields strongly influence these two quantities.

The outcomes have shown that this influence quantity does not necessarily imply a worsening in the performances of the LPCTs, but rather an inconstant behavior which is not influenced by the intensity of the harmonic distortion.

References

[1] Daher, N. A., Mougharbel, I., Saad, M., & Kanaan, H. Y. (2013). Comparative study of partitioning methods used for secondary voltage control in distributed power networks. Paper presented at the IEEE International Conference on Smart Energy Grid Engineering, SEGE 2013.

[2] Yang, L., & Quan, L. (2011). A topology control algorithm using power control for wireless mesh network. Paper presented at the Proceedings - 3rd International Conference on Multimedia Information Networking and Security, MINES 2011, 141-145.

[3] Mingotti, A., Peretto, L., & Tinarelli, R. (2018). Accuracy evaluation of an equivalent synchronization method for assessing the

time reference in power networks. IEEE Transactions on Instrumentation and Measurement, 67(3), 600-606.

[4] BS EN 50160:2010+A1. Voltage Characteristics of Electricity Supplied by Public Electricity Networks; BSI Standards Publication: London, UK, 2015.

[5] IEC 61869-6. Part 6: Additional general requirements for low-power instrument transformers. In Instrument Transformers; International Standardization Organization: Geneva, Switzerland, 2016.

[6] Malych, R., Barczi, O., & Vrabček, P. (2010). Characterization of a high current measurement system with rogowski current sensor. Paper presented at the 17th Symposium IMEKO TC4 - Measurement of Electrical Quantities, 15th International Workshop on ADC Modelling and Testing, and 3rd Symposium IMEKO TC19 - Environmental Measurements, 16-20.

[7] Cataliotti, A., Di Cara, D., Emanuel, A. E., Nuccio, S., & Tinè, G. (2011). Characterization and error compensation of a rogowski coil in the presence of harmonics. IEEE Transactions on Instrumentation and Measurement, 60(4).

[8] Mingotti, A., Peretto, L., & Tinarelli, R. (2020). Smart characterization of rogowski coils by using a synthetized signal. Sensors (Switzerland), 20(12), 1-16.

[9] Lisowiec, A., Nowakowski, A., & Kowalski, G. (2019). Operation of air core current transducers in the presence of strong interfering magnetic fields. Paper presented at the 2019 19th International Symposium on Electromagnetic Fields in Mechatronics, Electrical and Electronic Engineering, ISEF 2019.

[10] Mingotti, A., Peretto, L., & Tinarelli, R. (2020). Effects of multiple influence quantities on rogowski-coil-type current transformers. IEEE Transactions on Instrumentation and Measurement, 69(7).

[11] Xu, M., Yan, J., Geng, Y., Zhang, K., & Sun, C. (2018). Research on the factors influencing the measurement errors of the discrete rogowski coil. Sensors (Switzerland), 18(3).

[12] Xu, Y., Zou, X., & Wang, X. (2019). Influencing factors and error analysis of pulse current measurement with air-core rogowski coil. Paper presented at the IEEE International Pulsed Power Conference, 2019-June.

[13] IEC 61869-10. Part 10: Additional requirements for low-power passive current transformers. In Instrument Transformers; International Standardization Organization: Geneva, Switzerland, 2018.

[14] IEEE Std 519-2014, “Recommended Practice and Requirements for Harmonic Control in Electric Power Systems”, New York, USA, 2014.